ACS APPLIED MATERIALS & INTERFACES

Research Article

Cite This: ACS Appl. Mater. Interfaces 2018, 10, 12870−12877

www.acsami.org

High-Sensitivity and Low-Power Flexible Schottky Hydrogen Sensor Based on Silicon Nanomembrane

Minkyu Cho, Jeonghoon Yun, Donguk Kwon, Kyuyoung Kim, and Inkyu Park*

Department of Mechanical Engineering and KI for NanoCentury, KAIST, Daejeon 34141, Republic of Korea

Supporting Information

ABSTRACT: High-performance and low-power flexible Schottky diode-based hydrogen sensor was developed. The sensor was fabricated by releasing Si nanomembrane (SiNM) and transferring onto a plastic substrate. After the transfer, palladium (Pd) and aluminum (Al) were selectively deposited as a sensing material and an electrode, respectively. The top-down fabrication process of flexible Pd/SiNM diode H_2 sensor is facile compared to other existing bottom-up fabricated flexible gas sensors while showing excellent H_2 sensitivity ($\Delta I/I_0$ > 700−0.5% H_2 concentrations) and fast response time (τ_{10-90} = 22 s) at room temperature. In addition, selectivity, humidity, and mechanical tests verify that the sensor has excellent reliability and robustness under various environments. The operating power consumption of the sensor is only in the nanowatt range, which indicates its potential applications in low-power portable and wearable electronics.

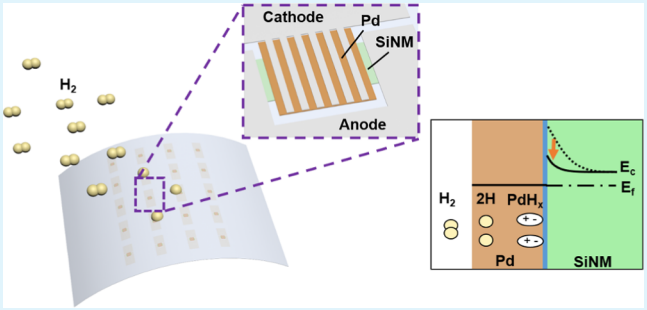

KEYWORDS: *hydrogen sensor, Schottky diode, palladium, silicon nanomembrane, flexible gas sensor, low-power gas sensor*

INTRODUCTION

Hydrogen (H_2) is useful as a future clean energy resource and an ideal replacement for the fossil fuels. Unlike oil-derived internal combustible engines that emit harmful gases to human health, such as CO_2, NO_x, and volatile organic compounds,[1] H_2 fuel cells generate H_2O as a byproduct after the reaction of H_2 and O_2. Besides the usage as a replacement for fossil fuels, H_2 gas also has been used for various industrial applications, such as petroleum refining, glass purification, semiconductor manufacturing, and pharmaceutical processing. However, H_2 poses great danger because it is flammable at concentrations over 4% by volume. Therefore, it is crucial to detect the H_2 gas leakages promptly before any catastrophic event occurs, and the development of high-performance H_2 gas sensor with low cost is necessary.

Application of Si to flexible gas sensors with proper surface modifications has definite advantages because of high stability against humidity and other interferences, compatibility to current Si technology, and low fabrication cost. So far, various Si-based gas sensors had been reported in a rigid form.[2−11] Han et al. reported silicon nanowire-based chemical gated transistor decorated with tin oxide (SnO_2) film on top and demonstrated an operation of the sensor under 1 V for mobile application.[12] Fahad et al. demonstrated multiplexed gas sensors using 3.5 nm thin silicon transistors with different metal decorations. The multiplexed Si sensor was able to selectively detect H_2, hydrogen disulfide (H_2S), and nitrogen dioxide (NO_2).[13]

The technical advancement in materials and processing technologies adds flexibility and conformality to the existing sensor technology. Flexible H_2 gas sensors are useful in diverse applications, such as portable electronics and aerospace systems, that require light-weight and mechanical shock-resistive sensing elements.[14] Various flexible H_2 gas sensors were reported previously with different materials, device structures, and fabrication methods. Sun et al. reported a flexible H_2 sensor using carbon nanotube (CNT) with Pd nanoparticles decoration.[15] The sensor showed 55.3% sensitivity ($\Delta R/R_0$) to 0.1% H_2 concentration and was able to detect as low as 30 ppm with 3% sensitivity. Lim et al. reported flexible Pd-nanotube-based H_2 sensor.[16] To synthesize Pd nanotubes on a flexible substrate, zinc oxide (ZnO) nanotubes were directly grown as templates by hydrothermal method and Pd nanostructures were formed by the reduction of Pd precursor and in situ dissolution of ZnO nanotube templates. This sensor showed 1500% sensitivity ($\Delta R/R_0$) to 0.1% H_2 concentration at room temperature.[16] Shin et al. reported a flexible H_2 sensor based on Pd cluster-decorated graphene electrodes by electrodeposition method.[17]

In the paper, we report Si nanomembrane (SiNM)-based diode-type H_2 sensor. Several electrical and material characteristics of the devices based on SiNM have been introduced, such as flexible radio frequency thin-film transistors,[19,20] microwave switches,[21] and solar cell.[22] However, as of now, there is little investigation on how the electrical characteristics of SiNM-based device would be modulated for a H_2 sensor. To fabricate this sensor, SiNMs were released from rigid substrates and

Received: January 29, 2018
Accepted: March 26, 2018
Published: March 26, 2018

DOI: 10.1021/acsami.8b01583
ACS Appl. Mater. Interfaces 2018, 10, 12870−12877

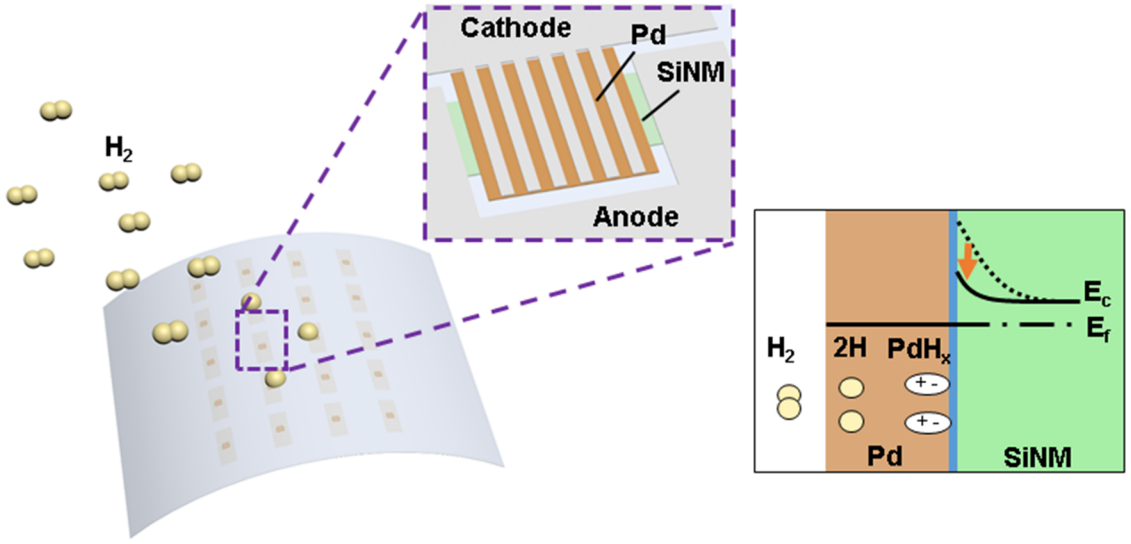

Figure 1. Graphical illustrations of flexible Pd/SiNM H_2 sensor (left) and energy bend diagram demonstrating the H_2 sensing mechanism. Cathode electrode is interdigitated to increase the reaction surface of Pd layer to H_2. Decomposed hydrogen atoms from H_2 gas molecules are diffused into the Pd layer and form dipoles (PdH_x) at Pd/SiNM interface, and Schottky barrier is lowered.

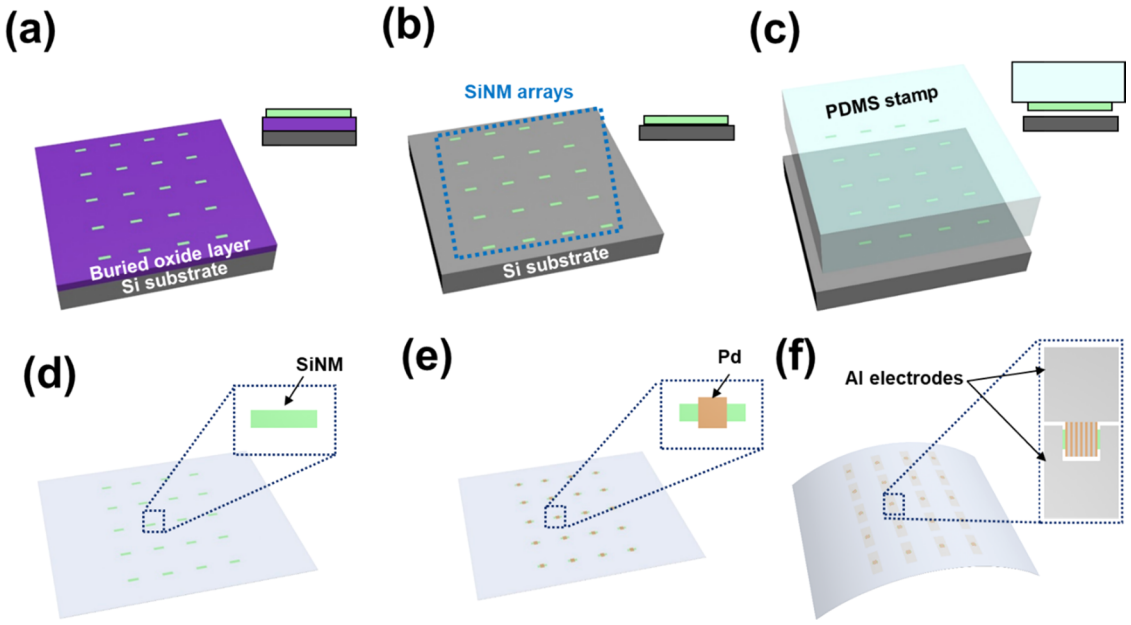

Figure 2. Graphical illustrations of flexible Pd/SiNM H_2 gas sensor after each fabrication process step: (a) selective RIE etching on a SOI substrate, (b) release of SiNM by BOE, (c) PDMS pickup of SiNM, (d) transfer of SiNM onto a plastic substrate, (e) Pd deposition, and (f) Al electrodes deposition.

directly transferred to flexible substrates, followed by metal depositions. The sensor fabrication process is facile and applicable to wafer-scale as compared with the current H_2 sensors based on chemically synthesized nanomaterials while having excellent gas-sensing performance. The measurement results show that the flexible SiNM diode gas sensor has a wide range of detection with high sensitivities to 50−5000 ppm H_2 concentrations consuming very low power (nanowatt range). In addition, the sensor showed a great selectivity to H_2 against other interfering gases and excellent sensing characteristics under mechanical bending conditions. Figure 1 shows graphical illustrations of the flexible Pd/SiNM H_2 sensor. As shown in Figure 1 (middle), the sensor is composed of SiNM and two contacts Pd and Al on a plastic substrate. Schottky barrier is formed at the Pd/Si interface. Upon the exposure to H_2 gas, H_2 molecules are dissociated into hydrogen atoms and the atoms are diffused into Pd layer forming palladium hydride (PdH_x) at the Pd/Si interface. PdH_x works as dipoles occupying interstitial states and lowers the Schottky barrier (Figure 1, right). The increased reverse current under H_2 exposure is a typical response for Schottky barrier lowering.[2,18,23,24]

EXPERIMENTAL WORK

Device Fabrication. The fabrication process is graphically explained in Figure 2a−f. The fabrication process started with an n-type silicon-on-insulator (SOI) wafer with a 50 nm thick top Si layer and 400 nm thick buried oxide (BOX) layer. The doping concentration of the top Si layer is 1×10^{18} cm^{-3}. The SOI wafer was patterned with positive photoresist (AZ 5214), and the top Si

DOI: 10.1021/acsami.8b01583
ACS Appl. Mater. Interfaces 2018, 10, 12870−12877

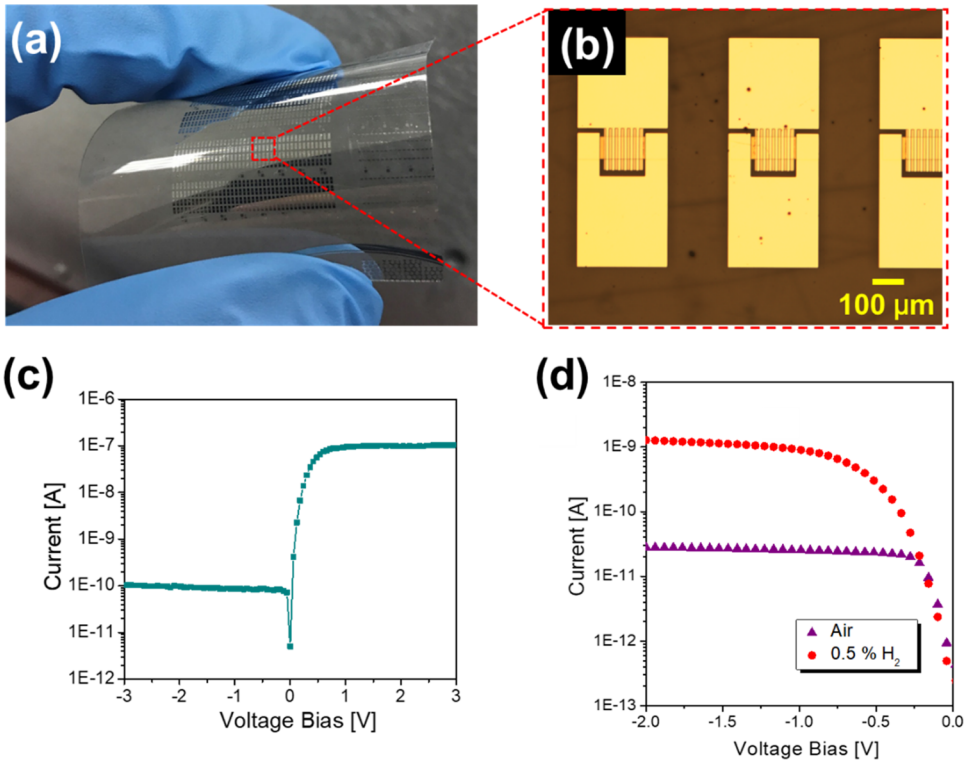

Figure 3. (a, b) Photographic and optical microscope image of flexible Pd/SiNM H_2 gas sensor; (c) $I-V$ characteristics of the sensor; and (d) current change in reverse bias before and after 0.5% H_2 exposure. On/off ratio is ~1000, and the change of the current under reverse bias is clearly shown during H_2 exposure.

layer was selectively etched by reactive ion etching (RIE) to define SiNM area, as shown in Figure 2a. The dimensions of a SiNM is 300 μm in length and 80 μm in width. After defining SiNM area, the sample was immersed in buffered oxide etching (BOE) solutions, as shown in Figure 2b. In this step, the SiNM was released by removing the BOX layer and bonded to the Si substrate by van der Waals force. The released SiNM was later picked up by a polydimethylsiloxane (PDMS) stamp and transferred to a SU-8-coated poly(ethylene terephthalate) (PET) substrate, as shown in Figure 2c,d. The photographic and optical microscopic images regarding SiNM transfer process can be found in Figure S5a,b. This transfer of SiNM is possible due to the stronger adhesion force between SU-8 and SiNM than the van der Waals force between the PDMS stamp and SiNM.[25] After the transfer, the PET substrate was exposed to UV light to permanently cure the SU-8 layer. Then, 20 nm thick palladium (Pd) and 200 nm thick aluminum (Al) were deposited by an electron beam evaporator as a sensing and an electrode material, respectively, as shown in Figure 2e,f. The Al electrode on the Pd side was designed as a comb structure for effective absorption of H_2 to the Pd surface.

Electrical Characterization and Gas-Sensing Experiment. The $I-V$ curve of the sensor was obtained by an Agilent 4155 semiconductor analyzer. For the gas experiment, the sensor was mounted in a sealed chamber with gas inlets and outlets. Each gas flow rate was controlled by mass flow controllers (MFCs), and the current response to H_2 gas of the sensor was measured at room temperature in real time by a Keithly 2635B current sourcemeter. Both MFCs and the current source were then controlled by the LabVIEW interface. For the humidity test, the relative humidity (RH) was controlled by changing the proportion of the humid air generated by saturated salt solution.

Mechanical Bending Test. For a repeated bending test, two three-dimensional (3D)-printed rounded tips mounted on a linear stage repeatedly bent the sensor by pressing down two edges of the sample, whereas the center of the sample was fixed on a cylinder block (20 mm radius curvature).

RESULTS AND DISCUSSION

The photograph and optical microscope images of the sensor are shown in Figure 3a,b. The current in Schottky diode based on diffusion current and thermionic emission can be written as

$$J_n = qvN_c \exp\left(-\frac{\phi_B}{V_t}\right)\left[\exp\left(\frac{V_a}{V_t}\right) - 1\right] \quad (1)$$

where q is the electron charge, v is the velocity, and N_c is the carrier density. Figure 3c shows the $I-V$ curve characteristic of the Pd/SiNM Schottky diode with on/off ratio ~1000. Upon the exposure to H_2 gas, the Schottky barrier height is lowered and the reverse bias current is increased.[2,23,24] The increase of the reverse current to 0.5% H_2 exposure is clearly seen in Figure 3d. The H_2 sensitivity was calculated as

$$\frac{I_{H_2} - I_{air}}{I_{air}} \times 100\ (\%) \quad (2)$$

where I_{air} is the current in air and I_{H_2} is the current in H_2 environment. Figure 4a shows the gas response at different voltage bias. For H_2 concentrations of 0.1, 0.3, and 0.5% and at −1 V bias, the gas responses were 197, 495, and 764%, respectively. As shown in Figure 4b, the sensitivity under forward bias was not observed because the forward current is large and not much affected by Schottky barrier height, whereas the H_2 sensitivity was clearly visible under reverse bias condition.

The general absorption/desorption behaviors of H_2 on Pd metal can be described by the Langmuir isotherm absorption theory.[26] On the basis of this theory, the absorption and desorption rates are described as $k_1 P_{H_2}(1-\theta)^2$ and $k_{-1}\theta^2$,

DOI: 10.1021/acsami.8b01583
ACS Appl. Mater. Interfaces 2018, 10, 12870−12877

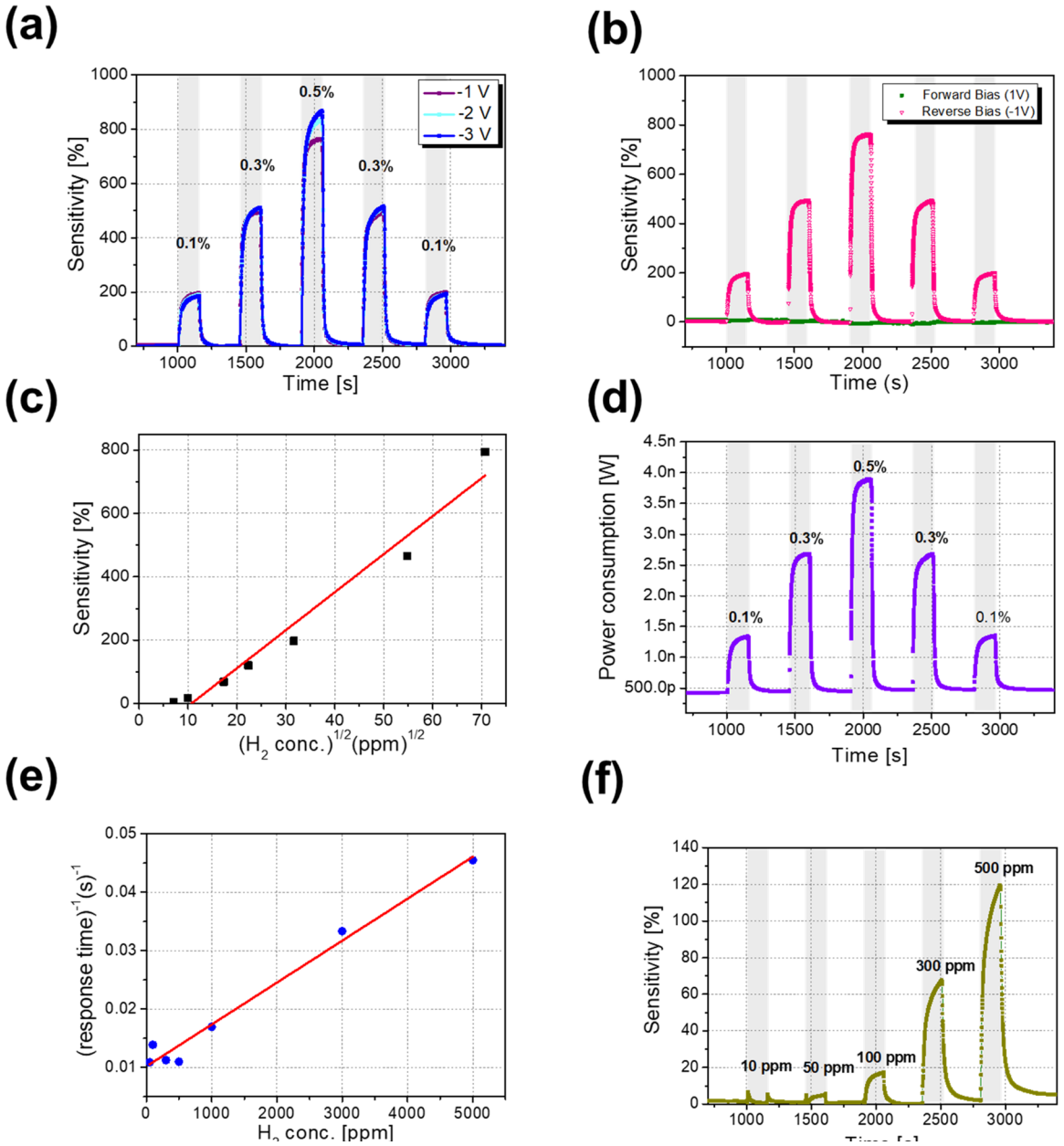

Figure 4. (a) H_2 sensitivity with different reverse bias voltage; (b) sensitivity vs H_2 concentration for different reverse voltage bias; (c) sensitivity vs the square root of H_2 concentration; (d) reciprocal of the response time vs H_2 concentration; (e) power consumption of the sensor; and (f) sensitivities in low H_2 concentrations (10−500 ppm).

where k_1 is the absorption constant, k_{-1} is the desorption constant, and θ is the H_2 coverage. When the absorption and desorption rates are equal, the equation

$$\left(\frac{\theta}{1-\theta}\right)^2 = \frac{k_1}{k_{-1}} P_{H_2} \tag{3}$$

is satisfied. Assuming that the P_{H_2} is low, $\theta/(1-\theta)$ term from eq 3 can be approximated to θ and $\Delta R/R$ is proportional to θ.[27] Therefore, eq 2 can be rewritten as

$$\frac{\Delta R}{R} \propto \theta = \sqrt{\frac{k_1}{k_{-1}}} \sqrt{P_{H_2}} \tag{4}$$

The sensitivity versus the square root of H_2 partial pressure was plotted and showed good linearity (R = 0.98), as shown in Figure 4c. Although this approximation (i.e., the linear relationship between resistance change and square root of partial pressure) is a good fit for most chemoresistive Pd-based H_2 sensors,[16,17,27] it neglects the amplifying effect of the gas sensor devices themselves. For example, the unusually high sensitivities of the diode and field-effect transistor (FET)-type gas sensors with external voltage-biased gates cannot simply be explained by the high absorption rate.[2,6] For the flexible Pd/SiNM diode H_2, the high sensitivity of the sensor to H_2 gas is due to the low reverse current and the modulation of Schottky barrier height.

The power consumptions of the device at a bias of −1 V in air are several hundreds of picowatts and reached up to several nanowatts when it was exposed to H_2 (Figure 4d). This power consumption of the device is very low compared to previously reported room-temperature Pd-decorated Si H_2 gas sensors.[6,7]

DOI: 10.1021/acsami.8b01583
ACS Appl. Mater. Interfaces 2018, 10, 12870−12877

Table 1. Performances of Flexible H_2 Sensors

type	sensor material	H_2 concn (%)	sensitivity (%)	response time (s)	tested bending radius	ref
diode	Pd, SiNM	0.5	764	22 s (10–90%)	ρ = 20 mm	this work
resistive	Pd nanotube	0.5	1800	80 s (10–90%)	ρ = 10 mm	16
resistive	Pd-decorated SWCNT	0.5	110	3 s (0–36.8%)	ρ = 7.5 mm	15
resistive	Pd-decorated ZnO	0.1	95	18 s (0–90%)	40 and 90° (unknown bending radius)	37
resistive	Pd-decorated graphene	0.1	33	~60 s (0–36.8%)	ρ = 3.5, 6.5 mm	38

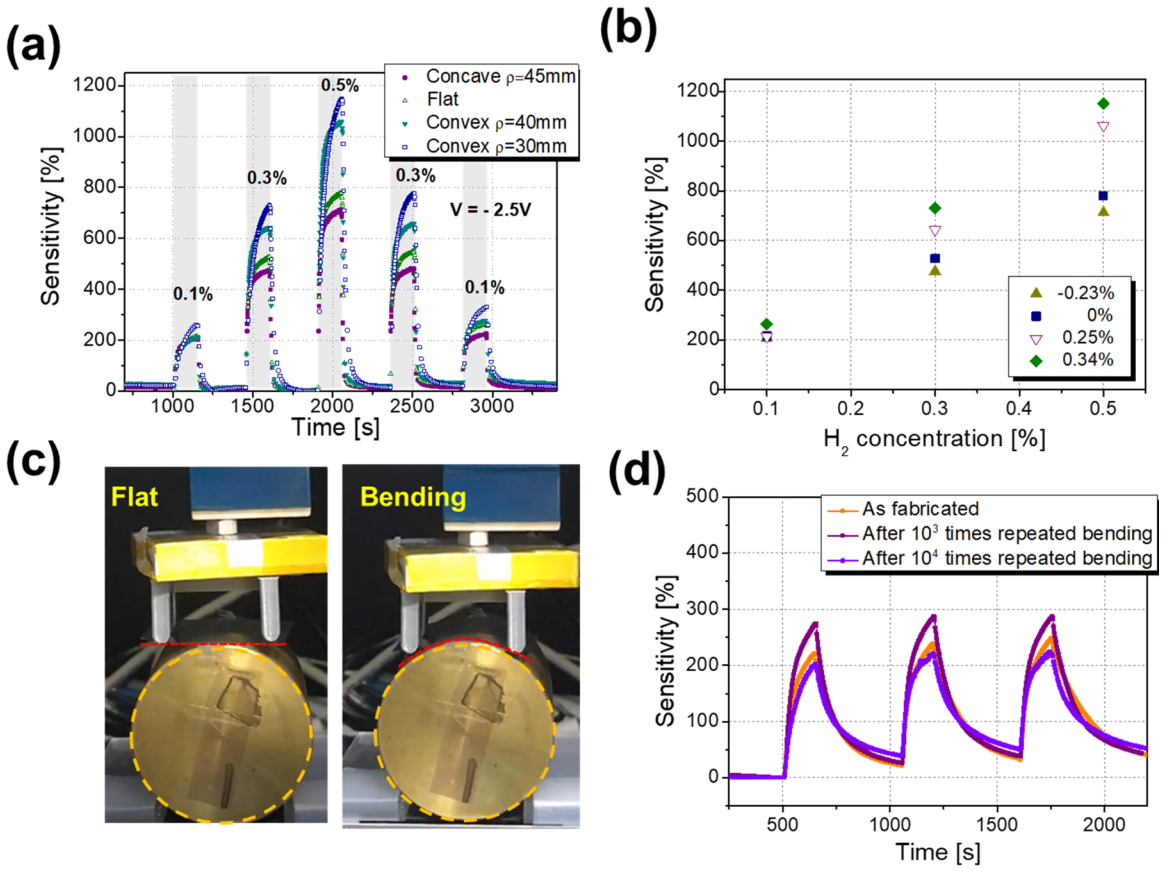

Figure 5. Sensor response under different degrees of mechanical strains: (a) real-time gas-sensing responses under different H_2 concentrations. (b) Sensitivity vs H_2 concentration for different mechanical strains. As more tensile strain is applied, the sensitivity is increased. This phenomenon is more pronounced as H_2 concentration is increased. Mechanical bending test of the sensor: (c) photographic images of the mechanical bending test setup and (d) H_2 sensitivity test results, after fabrication, 10^3, and 10^4 times of repeated bending. Insignificant degradation is observed after 10^4 repeated bending test.

Typical Pd-decorated FET sensors that have external gate operate in subthreshold regime to maximize their sensitivity to H_2 gas.[6] Likewise, working in the reverse bias regime, the power consumptions of the Pd/SiNM diode gas sensor during the standby/operation are significantly low. The response time was measured on the basis of the time interval in 10–90% of the maximum response to each gas concentration. Under −1 V bias, for H_2 concentrations of 0.1, 0.3, and 0.5%, the response times are 59, 30, and 22 s, respectively. The absorption rate, $r = k_1 P_{H_2}(1-\theta)^2$, can be approximated to $r = k_1 P_{H_2}$ when P_{H_2} is low. The reciprocal response time versus H_2 concentrations plotted in Figure 4e shows a linear relationship similar to the approximation. The gas test in lower H_2 concentrations was performed, as shown in Figure 4f. The measurable limit of detection (LOD) of the sensor was 50 ppm as shown in Figure S2, and the sensor was able to detect and distinguish low-concentration H_2 gases ranging from 50 to 500 ppm. The sensitivity to 10 ppm H_2 gas could not be measured, and this may be attributed to the limitation of our current experimental setup. The overall sensing performance of the Pd/SiNM diode H_2 gas sensor was compared with other reported flexible H_2 sensors in Table 1. The sensitivity of the sensor (764%) is not as high as that of Pd-nanotube flexible sensors (1800%), but it has shorter response time (22 s) to 0.5% H_2 concentrations with lower power consumption.

To observe the mechanical strain effects on the gas-sensor performances, the sensitivity of the sensor to H_2 gas under different degrees of bending was measured. For each measurement, the sensors were fixed on 3D-printed half-cylindrical blocks with different radii of curvature: 45 mm (concave), 40 mm (convex), and 30 mm (convex). The sensor was bent along ⟨110⟩ crystalline direction, the same as the current channel direction of the sensor. The strains are calculated on the basis of the equation[28]

DOI: 10.1021/acsami.8b01583
ACS Appl. Mater. Interfaces 2018, 10, 12870–12877

$$\text{strain}\ (\%) = \frac{1}{\frac{2\rho}{t} + 1} \quad (5)$$

where ρ is the radius of the fixture and t is the thickness of the bent object. On the basis of eq 5, we obtained strain values of −0.23, 0.25, and 0.34% of the sensor for the curvature radii of −45 mm (concave), 40 mm (convex), and 30 mm (convex), respectively. The gas responses to different H_2 concentrations and strains were shown in Figure 5a. In all tested gas concentrations, the gas sensitivities were increased as more tensile strains were applied. The reason for the increased response is ascribed to the enhanced carrier mobility of Si under tensile strain. It has been well known that the mechanical strain increases the carrier mobility in Si by splitting the 6-fold degeneracy into 2-fold and 4-fold degeneracy.[29] As a result, the effective mass and intervalley scattering are reduced. For SiNM, applying high degrees of mechanical strain is possible by bending the object while maintaining its single-crystalline properties.[30] Several researches have been reported on the mechanical strain effect of SiNM by mechanical bending.[28,31−33] In our Pd/SiNM diode H_2 gas sensor, it was found that the gas sensitivity was increased as tensile strain was increased, as shown in Figure 5b, in all tested gas concentrations. Similar effect had been reported previously. Qin et al. had reported SiNM-based flexible diode switch and shown that its switch characteristics in ON state was enhanced as tensile strain was increased because of the reduced intrinsic series resistance.[32] To understand the mechanism of the enhanced sensitivity of the Pd/SiNM diode sensor under mechanical strain, an equivalent circuit model was constructed as shown in Figure S3 and the calculation for the gas sensor sensitivity based on the equivalent circuit is explained in Supporting Information. According to the model, the rate of increased strain by applying strain is closely related to the ratio of the Schottky barrier resistance in air condition, $R_{sh.air}$, and the Schottky barrier resistance in H_2 gas, $R_{sh.gas}$. When $R_{sh.air} > R_{sh.gas}$, the response of the sensor depends on the change of R_{SiNM}. The rate of the sensitivity as R_{SiNM} is increased depends on the ratio between $R_{sh.air}$ and $R_{sh.gas}$, as shown in Figure S4. From the gas experiment, it can be conjectured that the ratio between $R_{sh.air}$ and $R_{sh.gas}$ is closely related to the gas concentration as well as the gas response. The response of the gas sensor for H_2 concentration of 0.1−0.5% is 197−764%. Considering the sensitivity range obtained from the gas experiment, the boundary condition could be estimated. Within the boundary condition, it was found that the reduced R_{SiNM} by increasing mobility upon tensile strain enhanced the gas response of the sensor. It should be noted that this phenomenon is only applied to SiNM across which the series resistance is sufficiently high compared to R_{sh}. More detail analysis will be carried out in future research. To investigate the mechanical reliability of our sensor, a repeated bending test was performed. The photographic images of the test setup are shown in Figure 5c, and a video recorded during the test is attached in Supporting Information. The repeated bending tests were composed of two sets: 10^3 times of repeated bending for the first set and additional 10^4 times for the second set. The substrate was bent along the curvature of the cylinder with 20 mm radius curvature. It should be noted that the main application of the sensor is to mount in reasonably curved surfaces. Considering the application, we believe the tested bending radius fit to its purpose. The detail of experimental conditions can be found in the Experimental Work section. After each set of repeated bending cycles, the gas-sensing characteristics were characterized. As shown in Figure 5b, the sensitivity has not been decreased after 10^3 times of repeated bending. Although minor decrease of sensitivity (by 9%) occurred after additional 10^4 times of repeated bending, the degradation of device performance was insignificant. On the basis of the calculated strain (0.50%) applied to the sensor during the repeated bending/relaxing test with 20 mm radius curvature and Young's modulus of Si (190 GPa), the stress applied to the SiNM sensor during the test could be estimated (950 MPa). This stress applied during the bending is about 14% of the known yield strength of Si (7 GPa),[34] indicating that the sensor can endure high cycles of repeated bending/relaxing without a mechanical failure. Moreover, both flexural rigidity and flexural strength are proportional to the reciprocal of the thickness.[35,36] Therefore, extremely high flexural strength and rigidity are expected in the small thickness (50 nm) of SiNM as compared to the rigid Si substrate (typical thickness > 200 μm).

To investigate the selectivity of the H_2 sensor, the responses of the sensor were measured for different types of gases: NO_2, CO, H_2S, and NH_3 (Figure 6). The limit of detection (LOD) for H_2 was 50 ppm in the current experimental setup, and the concentrations for each gas except for H_2 gas was set at 20 ppm for comparison, as shown in the graph in Figure 6. For NO_2, CO, and NH_3, the sensor showed low negative sensitivity (i.e., $\Delta I/I_0 < 0$). These gases are diffused into absorption sights of the sensor reducing the current across the sensor. The sensitivity to 20 ppm NO_2 is −85%, which was the highest among tested interfering gases. The sensitivities to 20, 100, and 160 ppm CO were −0.5, −0.9, and −4.8%, respectively. The sensitivity to 20 ppm NH_3 was −0.7%. On the other hand, positive sensitivity ($\Delta I/I_0 > 0$) was observed for H_2S gas similarly to H_2, and this might be due to partial decomposition of the H atoms in H_2S. In the selectivity measurement, one should consider effective hazardous concentration limit for each gas. According to Occupational Safety and Health Administration (OSHA), permissible exposure limits (PELs) for the test gases are 5 ppm (NO_2), 10 ppm (H_2S), 50 ppm (CO), and 50 ppm (NH_3). These limits are much lower than the lower

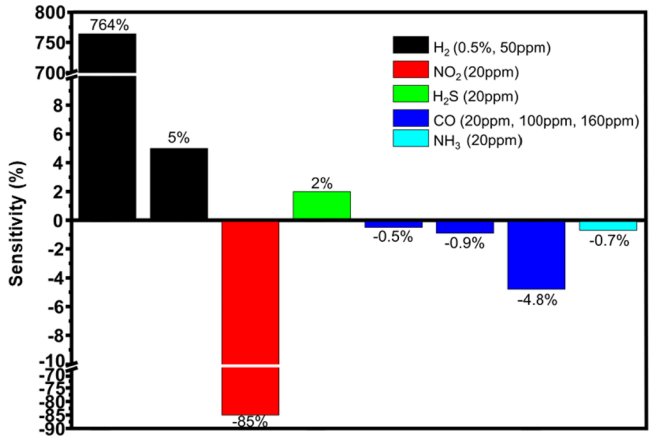

Figure 6. Response graph of the sensor upon various gas exposures: H_2 (0.5%, 50 ppm), H_2S (20 ppm), NO_2 (20 ppm), CO (20, 100, and 160 ppm), and NH_3 (20 ppm). Each gas concentration was set on the basis of the permissible exposure limits (PELs) by Occupational Safety and Health Administration (OSHA) and currently available gas sources.

DOI: 10.1021/acsami.8b01583
ACS Appl. Mater. Interfaces 2018, 10, 12870−12877

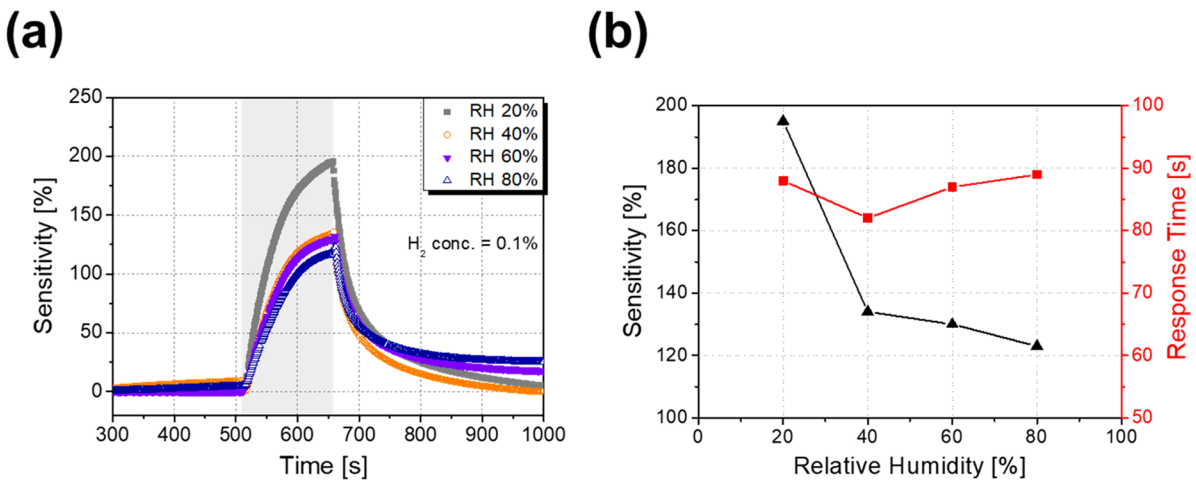

Figure 7. H_2 sensitivity of the sensor under different relative humidities: (a) sensitivity vs time, (b) sensitivity and response time vs relative humidity. Decrease in sensitivity is observed as relative humidity (RH) is increased from 20 to 40%, however, minor decrease in sensitivity is observed above RH 40%. Response time was less affected by humidity (20−80%).

explosive limit of H_2 (4%, 40 000 ppm). Considering the flammable range of H_2, the sensor showed good selectivity to H_2 over other interfering gases.

To understand the influence of humidity on the gas-sensor performances, the gas sensitivity and response time to 0.1% H_2 gas under different relative humidity (RH) conditions were measured, as shown in Figure 7a,b. In humid environment, water molecules are condensed on the surface of the absorption sites hindering the absorption of H atoms on the Pd surface.[7] As shown in Figure 7b, the maximum sensitivity of the gas sensor was decreased by 2% (from 197 to 195%) as RH was increased from 0 to 20%. At 40, 60, and 80% RH, the sensitivities were decreased to 134, 130, and 123%, respectively. Although the sensitivity was decreased by 61% as the humidity was increased from 20 to 40% RH, it did not show significant decreases in sensitivity above 40%. The response time was increased from 59 to 88 s as the RH was increased from 0 to 20%, but became less affected as the humidity was increased above 20% RH.

CONCLUSIONS

In summary, a flexible Pd/Si Schottky diode-based H_2 sensor was reported using SiNM transfer on a plastic substrate. The gas test for H_2 gas was performed, and it showed high H_2 sensitivity and short response time with low power consumption. The high sensitivity of the sensor is mainly due to the exponential current characteristic upon changing Schottky barrier height. The static mechanical strain effect on the sensing performance was observed by experiment. The sensitivity to other gas was tested, an excellent selectivity of the sensor to H_2 over other gases was confirmed. A repeated bending test was also performed to test its mechanical durability as a flexible sensor, and high sensitivity and stable device performance were maintained even after 10^4 times of repeated bending. The sensor fabrication process is mostly composed of standard complementary metal-oxide−semiconductor process meaning that it is easily applicable to wafer-scale. In conjunction with other types of sensors, such as temperature, humidity, and pressure, this high-performance and low-power Pd/SiNM diode sensor with a simple fabrication process would be useful in the future flexible/wearable electronics with low cost.

ASSOCIATED CONTENT

Supporting Information

The Supporting Information is available free of charge on the ACS Publications website at DOI: 10.1021/acsami.8b01583.

Depletion width calculation of the Pd−Si junction using full depletion approximation; calculation for the gas-sensor sensitivity based on a series resistance model; and Figures S1−S7 (PDF)

Mechanical reliability test movie (AVI)

AUTHOR INFORMATION

Corresponding Author

*E-mail: inkyu@kaist.ac.kr.

ORCID

Minkyu Cho: 0000-0002-0006-2063

Inkyu Park: 0000-0001-5761-7739

Notes

The authors declare no competing financial interest.

ACKNOWLEDGMENTS

This work was supported by the National Research Foundation of Korea (NRF) Grant funded by the Korean Government (MSIP) (No. 2015R1A5A1037668) and Nano Material Technology Development Program (2015M3A7B7045518) through the National Research Foundation of Korea (NRF) funded by the Ministry of Science, ICT & Future Planning.

REFERENCES

(1) Offer, G. J.; Howey, D.; Contestabile, M.; Clague, R.; Brandon, N. P. Comparative Analysis of Battery Electric, Hydrogen Fuel Cell and Hybrid Vehicles in a Future Sustainable Road Transport System. *Energy Policy* **2010**, *38*, 24−29.

(2) Fang, Y. K.; Hwang, S. B.; Lin, C. Y.; Lee, C. C. Trench Pd/Si Metal-oxide-semiconductor Schottky Barrier Diode for a High Sensitivity Hydrogen Gas Sensor. *Appl. Phys. Lett.* **1990**, *57*, 2686−2688.

(3) Fonash, S. J.; Huston, H.; Ashok, S. Conducting MIS Diode Gas Detectors: The Pd/SiOx/Si Hydrogen Sensor. *Sens. Actuators* **1981**, *2*, 363−369.

(4) Zhang, W.; de Vasconcelos, E. A.; Uchida, H.; Katsube, T.; Nakatsubo, T.; Nishioka, Y. A Study of Silicon Schottky Diode

DOI: 10.1021/acsami.8b01583
ACS Appl. Mater. Interfaces 2018, 10, 12870−12877

Structures for NOx Gas Detection. *Sens. Actuators, B* **2000**, *65*, 154−156.
(5) Ali, N. K.; Hashim, M. R.; Aziz, A. A. Effects of Surface Passivation in Porous Silicon as H_2 Gas Sensor. *Solid-State Electron.* **2008**, *52*, 1071−1074.
(6) Ahn, J.-H.; Yun, J.; Choi, Y.-K.; Park, I. Palladium Nanoparticle Decorated Silicon Nanowire Field-Effect Transistor with Side-gates for Hydrogen Gas Detection. *Appl. Phys. Lett.* **2014**, *104*, No. 013508.
(7) Ahn, J.-H.; Yun, J.; Moon, D.-I.; Choi, Y.-K.; Park, I. Self-heated Silicon Nanowires for High Performance Hydrogen Gas Detection. *Nanotechnology* **2015**, *26*, No. 095501.
(8) Nienhaus, H.; Bergh, H. S.; Gergen, B.; Majumdar, A.; Weinberg, W. H.; McFarland, E. W. Selective H Atom Sensors Using Ultrathin Ag/Si Schottky Diodes. *Appl. Phys. Lett.* **1999**, *74*, 4046−4048.
(9) Demarne, V.; Grisel, A. An Integrated Low-power Thin-film CO Gas Sensor on Silicon. *Sens. Actuators* **1988**, *13*, 301−313.
(10) Lundström, K. I.; Shivaraman, M. S.; Svensson, C. M. A Hydrogen-sensitive Pd-gate MOS Transistor. *J. Appl. Phys.* **1975**, *46*, 3876−3881.
(11) Yun, J.; Jin, C. Y.; Ahn, J.-H.; Jeon, S.; Park, I. A Self-heated Silicon Nanowire Array: Selective Surface Modification with Catalytic Nanoparticles by Nanoscale Joule Heating and Its Gas Sensing Applications. *Nanoscale* **2013**, *5*, 6851−6856.
(12) Han, J.-W.; Rim, T.; Baek, C.-K.; Meyyappan, M. Chemical Gated Field Effect Transistor by Hybrid Integration of One-Dimensional Silicon Nanowire and Two-Dimensional Tin Oxide Thin Film for Low Power Gas Sensor. *ACS Appl. Mater. Interfaces* **2015**, *7*, 21263−21269.
(13) Fahad, H. M.; Shiraki, H.; Amani, M.; Zhang, C.; Hebbar, V. S.; Gao, W.; Ota, H.; Hettick, M.; Kiriya, D.; Chen, Y.-Z.; Chueh, Y.-L.; Javey, A. Room Temperature Multiplexed Gas sensing Using Chemical-sensitive 3.5-nm-thin Silicon Transistors. *Sci. Adv.* **2017**, *3*, No. e1602557.
(14) Sun, Y.; Wang, H. H. High-Performance, Flexible Hydrogen Sensors That Use Carbon Nanotubes Decorated with Palladium Nanoparticles. *Adv. Mater.* **2007**, *19*, 2818−2823.
(15) Sun, Y.; Wang, H. H. Electrodeposition of Pd nanoparticles on Single-walled Carbon Nanotubes for Flexible Hydrogen Sensors. *Appl. Phys. Lett.* **2007**, *90*, No. 213107.
(16) Lim, M. A.; Kim, D. H.; Park, C.-O.; Lee, Y. W.; Han, S. W.; Li, Z.; Williams, R. S.; Park, I. A New Route toward Ultrasensitive, Flexible Chemical Sensors: Metal Nanotubes by Wet-Chemical Synthesis along Sacrificial Nanowire Templates. *ACS Nano* **2012**, *6*, 598−608.
(17) Shin, D. H.; Lee, J. S.; Jun, J.; An, J. H.; Kim, S. G.; Cho, K. H.; Jang, J. Flower-like Palladium Nanoclusters Decorated Graphene Electrodes for Ultrasensitive and Flexible Hydrogen Gas Sensing. *Sci. Rep.* **2015**, *5*, No. 12294.
(18) Card, H. C.; Rhoderick, E. H. Studies of Tunnel MOS Diodes I. Interface Effects in Silicon Schottky diodes. *J. Phys. D: Appl. Phys.* **1971**, *4*, 1589−1601.
(19) Sun, L.; Qin, G.; Seo, J.-H.; Celler, G. K.; Zhou, W.; Ma, Z. 12-GHz Thin-Film Transistors on Transferrable Silicon Nanomembranes for High-Performance Flexible Electronics. *Small* **2010**, *6*, 2553−2557.
(20) Zhou, H.; Seo, J.-H.; Paskiewicz, D. M.; Zhu, Y.; Celler, G. K.; Voyles, P. M.; Zhou, W.; Lagally, M. G.; Ma, Z. Fast Flexible Electronics with Strained Silicon Nanomembranes. *Sci. Rep.* **2013**, *3*, No. 1291.
(21) Qin, G.; Yuan, H.-C.; Celler, G. K.; Ma, J.; Ma, Z. RF model of flexible microwave switches Employing Single-crystal Silicon Nanomembranes on a Plastic Substrate. *Microelectron. Eng.* **2012**, *95*, 21−25.
(22) Yoon, J.; Baca, A. J.; Park, S.-I.; Elvikis, P.; Geddes, J. B.; Li, L.; Kim, R. H.; Xiao, J.; Wang, S.; Kim, T.-H.; Motala, M. J.; Ahn, B. Y.; Duoss, E. B.; Lewis, J. A.; Nuzzo, R. G.; Ferreira, P. M.; Huang, Y.; Rockett, A.; Rogers, J. A. Ultrathin Silicon Solar Microcells for Semitransparent, Mechanically Flexible and Microconcentrator Module Designs. *Nat. Mater.* **2008**, *7*, 907−915.
(23) Ruths, P. F.; Ashok, S.; Fonash, S. J.; Ruths, J. M. A Study of Pd/Si MIS Schottky Barrier Diode Hydrogen Detector. *IEEE Trans. Electron Devices* **1981**, *28*, 1003−1009.
(24) Skucha, K.; Fan, Z.; Jeon, K.; Javey, A.; Boser, B. Palladium/silicon Nanowire Schottky Barrier-based Hydrogen sensors. *Sens. Actuators, B* **2010**, *145*, 232−238.
(25) Carlson, A.; Wang, S.; Elvikis, P.; Ferreira, P. M.; Huang, Y.; Rogers, J. A. Active, Programmable Elastomeric Surfaces with Tunable Adhesion for Deterministic Assembly by Transfer Printing. *Adv. Funct. Mater.* **2012**, *22*, 4476−4484.
(26) Laidler, K. J. *Chemical Kinetics*; McGraw-Hill Book Company: New York, 1965.
(27) Rumiche, F.; Wang, H. H.; Hu, W. S.; Indacochea, J. E.; Wang, M. L. Anodized Aluminum Oxide (AAO) Nanowell Sensors for Hydrogen Detection. *Sens. Actuators, B* **2008**, *134*, 869−877.
(28) Qin, G.; Yang, L.; Seo, J.-H.; Yuan, H.-C.; Celler, G. K.; Ma, J.; Ma, Z. Experimental Characterization and Modeling of the Bending Strain Effect on Flexible Microwave Diodes and Switches on Plastic Substrate. *Appl. Phys. Lett.* **2011**, *99*, No. 243104.
(29) Mistry, K.; Armstrong, M.; Auth, C.; Cea, S.; Coan, T.; Ghani, T.; Hoffmann, T.; Murthy, A.; Sandford, J.; Shaheed, R.; Zawadzki, K.; Zhang, K.; Thompson, S.; Bohr, M. In *Delaying Forever: Uniaxial Strained SiliconTransistors in a 90nm CMOS Technology, Digest of Technical Papers*, 2004 Symposium on VLSI Technology; IEEE, 2004; pp 50−51.
(30) Lagally, M. G. Silicon Nanomembranes. *MRS Bull.* **2007**, *32*, 57−63.
(31) Feng, C.; Chanan, E.; Zheng, L.; Himpsel, F. J.; Feng, L.; Max, G. L. Conduction band structure and electron mobility in uniaxially strained Si via externally applied strain in nanomembranes. *J. Phys. D: Appl. Phys.* **2011**, *44*, No. 325107.
(32) Qin, G.; Yuan, H.-C.; Celler, G. K.; Ma, J.; Ma, Z. Impact of Strain on Radio Frequency Characteristics of Flexible Microwave Single-crystalline Silicon Nanomembrane P-intrinsic-n Diodes on Plastic Substrates. *Appl. Phys. Lett.* **2010**, *97*, No. 233110.
(33) Cho, M.; Seo, J.-H.; Park, D.-W.; Zhou, W.; Ma, Z. Capacitance-voltage Characteristics of Si and Ge Nanomembrane based Flexible Metal-oxide-semiconductor Devices under Bending Conditions. *Appl. Phys. Lett.* **2016**, *108*, No. 233505.
(34) Madou, M. *Fundamentals of Microfabrication*; CRC Press, 1997.
(35) Rogers, J. A.; Lagally, M. G.; Nuzzo, R. G. Synthesis, Assembly and Applications of Semiconductor Nanomembranes. *Nature* **2011**, *477*, 45−53.
(36) Junior, S. A. R.; Ferracane, J. L.; Bona, Á. D. Flexural strength and Weibull analysis of a Microhybrid and a Nanofill Composite Evaluated by 3- and 4-point Bending Tests. *Dent. Mater.* **2008**, *24*, 426−431.
(37) Rashid, T.-R.; Phan, D.-T.; Chung, G.-S. A Flexible Hydrogen Sensor Based on Pd Nanoparticles Decorated ZnO Nanorods Grown on Polyimide Tape. *Sens. Actuators, B* **2013**, *185*, 777−784.
(38) Chung, M. G.; Kim, D.-H.; Seo, D. K.; Kim, T.; Im, H. U.; Lee, H. M.; Yoo, J.-B.; Hong, S.-H.; Kang, T. J.; Kim, Y. H. Flexible Hydrogen Sensors Using Graphene with Palladium Nanoparticle Decoration. *Sens. Actuators, B* **2012**, *169*, 387−392.

DOI: 10.1021/acsami.8b01583
ACS Appl. Mater. Interfaces 2018, 10, 12870−12877